Retracted article: Electrochemical hydrogen production in aqueous micellar solution by a diiron benzenedithiolate complex relevant to [FeFe] hydrogenases

François Quentel, Guillaume Passard and Frederic Gloaguen

Phys. Chem. Chem. Phys., 2012, DOI: 10.1039/c2cp40085e). ***Retraction published 1st March 2012.***

We, the named authors, hereby wholly retract this Physical Chemistry Chemical Physics article.

Signed: François Quentel, Guillaume Passard and Frederic Gloaguen, France, March 2012.

Retraction endorsed by Philip Earis, Managing Editor. Retraction published 1st March 2012.

PCCP

Dynamic Article Links

Cite this: DOI: 10.1039/c2cp40085e

www.rsc.org/pccp

PAPER

Electrochemical hydrogen production in aqueous micellar solution by a diiron benzenedithiolate complex relevant to [FeFe] hydrogenases†

François Quentel, Guillaume Passard and Frederic Gloaguen*

Received 10th January 2012, Accepted 11th January 2012
DOI: 10.1039/c2cp40085e

The diiron hydrogenase model $Fe_2(bdt)(CO)_6$ (**1**, bdt = benzenedithiolate) was dispersed in aqueous micellar solution prepared from sodium dodecyl sulfate (SDS). Aqueous solution of **1** showed no sign of decomposition when left in contact with air over a period of several days. Current–potential responses recorded at a dropping mercury electrode over pH 7–3 were consistent with reduction of freely diffusing species. Catalysis of proton reduction was observed at pH < 6 with current densities exceeding 0.5 mA cm^{-2} at an acid-to-catalyst ratio of 17. Bulk electrolysis at −0.66 V *vs.* SHE of solution of **1** at pH 3 confirmed the production of hydrogen with a Faradaic efficiency close to 100%. A mechanism involving initial reduction of **1** and subsequent proton-coupled electron transfer is proposed.

1. Introduction

A basic limitation to large-scale production of molecular hydrogen (H_2) by photochemical and electrochemical water splitting is the lack of catalysts based on cheap and abundant material.[1–5] Catalysis of proton reduction by cobalt and nickel compounds has been extensively studied.[6–8] However, the natural abundance of these two transition metals is rather low (20 ppm and 90 ppm, respectively) as compared to iron (6.3%). Inspiration for the design of iron-based catalysts might be provided by the FeFe-hydrogenases ([FeFe]-H_2ases), a class of enzymes catalyzing the production of H_2 at high rates.[9,10] Indeed the active site of these enzymes contains a Fe_2S_2 core that has inspired, over the last decade, the synthesis of numerous structural and functional models of the type $Fe_2(SR)_2(CO)_6$ (Scheme 1).[11–14] While the use of water as a proton source for H_2 production is highly desirable, the lack of solubility of the majority of the [FeFe]-H_2ase models in aqueous media limited their study to organic solvents.[15] In an attempt to solve this issue, polymers functionalized with a diiron model complex were grafted on electrodes, but they showed poor catalytic activity.[16] On the other hand, few diiron models holding hydrophilic ligands were prepared, which permitted us to confirm the stability and activity of this type of catalyst in mixtures of organic solvent and water.[17–19] A recent report from Darensbourg and co-workers described the synthesis of sulfonated diiron derivatives that could be included in β-cyclodextrin.[20,21] This approach solves the problem of water solubility and offers moreover the possibility of mimicking the protein environment of the H_2ases. Unfortunately, addition of β-cyclodextrin tends to hinder the electrochemical activation of proton reduction by the diiron catalyst on a glassy carbon electrode. A few studies concerning photodriven H_2 production by diiron models in aqueous solution containing or not a fraction of organic solvents were also recently reported.[22,23] In particular, Wu and coworkers showed that water-insoluble diiron models and photosensitizers could be incorporated into micelles formed in an aqueous sodium dodecyl sulfate (SDS) solution.[24] This system produces H_2 with low rates using ascorbic acid as a sacrificial electron donor. However, the catalytic properties of the diiron models were not independently evaluated in aqueous SDS solution. Whether the H_2 production rate is limited by the activity of the catalyst, the coupling with the photosensitizer, or any other step was therefore not established. While micelles formed by surfactants in water are simple models of biological membranes, much of their interest relates to the possibility of dispersing a water-insoluble substance into a medium that is overall an aqueous one.[25] In particular, electrochemical data for a variety of organic molecules and transition

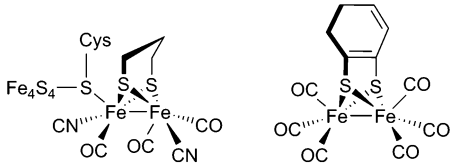

Scheme 1 Structures of the [FeFe]-H_2ase active site (left) and of the diiron model **1** (right).

UMR 6521, CNRS, Université de Bretagne Occidentale, 6 Av Le Gorgeu, Brest, France. E-mail: fgloague@univ-brest.fr; Fax: +33 298 017001; Tel: +33 298 017254

† Electronic supplementary information (ESI) available: Experimental details of UV-visible absorption measurements and electrochemical experiments including voltammograms at a glassy carbon electrode and charge build-up *vs.* time plots for bulk electrolysis on a mercury pool electrode. See DOI: 10.1039/c2cp40085e

metal complexes in an aqueous electrolyte could be obtained by dispersion in micelles. Electrochemical studies of water-insoluble substances moreover showed that micelle systems are able to stabilize reactive intermediates in aqueous solution.

In view of these previous results, we focused on electrochemistry of the water-insoluble diiron model $Fe_2(bdt)(CO)_6$ (**1**, bdt = benzenedithiolate, Scheme 1) dispersed in aqueous SDS solutions. Compound **1** was chosen because it is an air-stable binuclear iron(I) species.[26] Besides, it holds a bdt-bridging ligand that helps maintaining the integrity of the Fe_2S_2 core in the reduced iron(0) states.[27] Previous works from our laboratory showed that **1** is actually a robust but qnot very active catalyst for the reduction at mild potential of organic acid in non-aqueous solvents.[28,29] Herein, we demonstrate that **1** in aqueous SDS solutions is in contrast an active H_2 production catalyst operating at potentials positive to −0.7 V *vs.* SHE at pH ≈ 3.

2. Experimental

$Fe_2(bdt)(CO)_6$ (**1**) was prepared in moderate yield from reaction of $Fe_3(CO)_{12}$ with 1,2-benzenedithiol by slight modification of previously reported procedures.[30] Analytical grade chemicals and Milli-Q water were used in the preparation of aqueous solutions. To prepare aqueous solution of **1**, it was more convenient to dissolve the compound in a little methanol and then to dilute the resulting solution in water. In our experiments, the final concentration of methanol in water was lower than 0.25% v/v and had no detectable effect upon the results. Addition of SDS above the critical micellar concentration (10 mM) was however required to obtain aqueous solutions of **1** that did not look clouded at concentrations relevant to catalysis. Absorption spectra were recorded in quartz cells in contact with air on a Jasco V-670 Spectrophotometer. Current–potential responses of N_2-purged solutions of **1** were recorded unless otherwise noted on a dropping mercury electrode of 0.0052 cm^2 using a Metrohm VA 663 Stand. The reference electrode was a commercial Ag/AgCl, 3 M KCl electrode and the potentials are reported with respect to SHE by adding 0.208 V to the experimentally obtained values. Bulk electrolysis of 10 mL of solution of **1** was carried out at controlled potential on a stirred mercury pool of about 7 cm^2, while the Pt counter electrode was separated from the working electrode compartment by a fine porosity glass frit of about 0.2 cm^2. Faradaic efficiency was determined by pH increase measured with a glass electrode connected to an Orion Research pH/millivolt-meter model 811. The presence of H_2 in the electrolysis cell headspace was confirmed by analysis on a Varian 3900 Gas Chromatograph equipped with a TCD and a Porapak Q80/100 column (2 m × 1/8 in) using N_2 as a vector gas.

3. Results and discussion

3.1. UV-visible spectra of aqueous solution of 1

The absorbance spectrum of **1** in phosphate buffer solution at neutral pH shows an intense peak at 346 nm (ε = 7230 M^{-1} cm^{-1}) and a broad shoulder at 485 nm (Fig. 1).

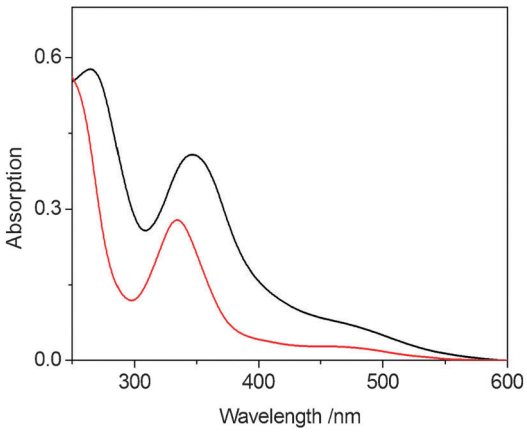

Fig. 1 UV-visible absorption spectra of 32 μM $Fe_2(bdt)(CO)_6$ (**1**) in 0.1 M phosphate buffer solution at pH 6.8 before (black trace) and after (red trace) addition of 10 mM SDS.

These features are similar to those of comparable diiron dithiolate complexes.[31] Addition of SDS gradually shifts the absorption bands towards the UV region. Once the critical micellar concentration is reached the absorption spectra become independent of SDS concentration ([SDS] ≥ 10 mM, λ_{max} = 335 nm, ε = 9530 M^{-1} cm^{-1}), suggesting an interaction of **1** with the micelles. Absorbance at λ_{max} obeys Beer's law for [**1**] ≤ 0.2 mM showing that the diiron compound is well dispersed in SDS aqueous solution at concentrations relevant to catalysis (Fig. S1, ESI†). Decreasing the pH of the solution has no noticeable influence on the absorption spectra, indicating that **1** does not react with protons at pH > 3 (Table S1, ESI†).[32] Interestingly, compound **1** shows no visible sign of degradation in solutions left in contact with air over a period of several days, as confirmed by UV-visible spectroscopy and electrochemistry.

3.2. Polarography of aqueous solutions of 1

Compound **1** exhibits a chemically reversible two-electron reduction in organic solvents. The reduced species $\mathbf{1}^{2-}$ reacts with strong organic acid (pK_a < 20) to catalytically produce H_2.[28,29] As we wanted to know whether a similar mechanism could occur in water, electrochemistry of aqueous SDS solutions of **1** was investigated at neutral and acid pH. Additionally, current–potential curves were recorded at a *dropping* mercury electrode to avoid strong adsorption of **1** and SDS observed with the glassy carbon electrode (Fig. S2, ESI†).

Polarograms of **1** at neutral pH show a primary reduction step at $E_{1/2}$ = −0.74 V (half-wave potential; all potentials are referenced to SHE, Fig. 2), a potential consistent with the mild reduction of the bdt-diiron derivatives in organic solvent.[28,29] We also note that this potential value is about 0.6 V less negative than those reported for the reduction in water of diiron models bearing hydrophilic ligands.[17–19] Linear dependence of the cathodic current on [**1**] moreover indicates the reduction of a free-diffusing species, confirming that there is no adsorption on the electrode. Primary reduction of **1** is followed by a second reduction event at about −0.90 V preceding a sharp rise in current at −1.05 V, suggesting catalytic reduction of water by a reduced form of **1** (*vide infra*). In organic solvents, compound **1** is reduced to its dianion in a chemically reversible two-electron process.

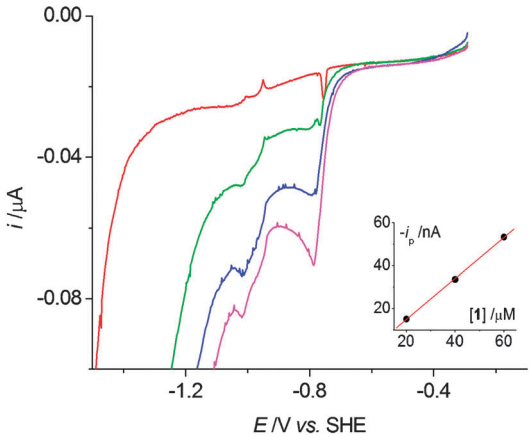

Fig. 2 dc-polarograms (scan rate: 2.5 mV s^{-1}) of 20, 40 and 60 μM **1** in 0.1 M NaCl containing 10 mM SDS and 10 mM phosphate buffer (pH 6.7). The red trace corresponds to the background current.

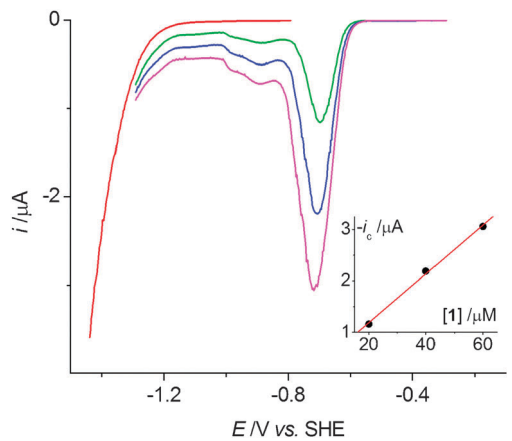

Fig. 3 dc-polarograms (scan rate: 2.5 mV s^{-1}) of 20, 40 and 60 μM **1** in 0.1 M NaCl containing 10 mM SDS and 10 mM acetic acid (pH 3.3). The red trace corresponds to the background current.

However, the number of electrons involved in the reduction of **1** at neutral pH cannot be estimated from the polarograms presented here because we suspect that the reduction of **1** is coupled to a protonation step.

Polarograms of **1** recorded in the presence of 10 mM acetic acid (HOAc) show a sharp current increase at a potential slightly less negative than that of the primary reduction of **1** at neutral pH (Fig. 3). The reduction of acid on the mercury electrode occurs at potentials more negative than −1.2 V. The current increase is therefore due to catalytic reduction of acid mediated by **1**. From the peak current value, we calculated a current density exceeding 0.5 mA cm^{-2} for [**1**] = 60 μM and [acid]/[**1**] = 17. Additionally, the catalytic current depends linearly on [**1**] demonstrating that homogeneous catalysis does occur.

Control experiments were carried out to confirm the catalytic activity of **1**. Polarograms of $Fe(SO_4)$ in SDS solution at neutral pH show that the reduction of Fe^{2+} occurs at a potential about 0.4 V more negative than that of **1**. The cathodic current is moreover poorly responsive to pH (Fig. S3, ESI†), indicating that the low valence iron species formed upon reduction of Fe^{2+} are not able to catalyse proton reduction.

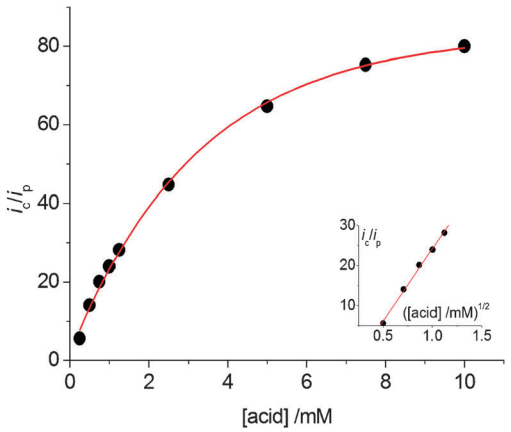

Fig. 4 Plot of the ratio of the catalytic current (i_c) to the peak current at neutral pH (i_p) *versus* the concentration of acetic acid measured for 20 μM **1** in 0.1 M NaCl containing 10 mM SDS.

A plot of the ratio of the catalytic current (i_c) to the current for the reduction of **1** at neutral pH (i_p) *versus* the acid concentration is shown in Fig. 4. Addition of acetic acid results in a substantial current enhancement that depends linearly on $[HOAc]^{1/2}$, suggesting that reaction is first order in acid as seen in organic solvents.[29] At higher acid concentration, the current enhancement levels off, eventually reaching a maximum $i_c/i_p = 80$ at acid concentrations above 5 mM (the acid-independent region). It is noteworthy that a significantly lower current enhancement ($i_c/i_p < 3$) was measured in acetonitrile in the presence of a large excess of toluenesulfonic acid as a proton source (Table S3, ESI†).

Dubois and co-workers[33] proposed a method for evaluating the turnover frequency (TOF) of a catalyst from the maximum of current enhancement in the acid-independent region. Unfortunately, this method implies measurements at increasing scan rates, which cannot be done at a *dropping* mercury electrode. Voltammetry at a *hanging* mercury electrode showed that the maximum of current enhancement becomes independent of the scan rate above 50 mV s^{-1} (Fig. S4, ESI†). The value $i_c/i_p \approx 120$ measured at $\nu = 100$ mV s^{-1} is in good agreement with the slightly lower value of 80 measured at 2.5 mV s^{-1} with a dropping mercury electrode under otherwise similar conditions ([**1**] = 20 μM, [HOAc] = 10 mM, Fig. 4). According to Dubois, the catalytic current enhancement (i_c/i_p) is related to the catalyst turnover frequency by: $TOF = 1.93 \times \nu \times (i_c/i_p)^2$. The value calculated here, TOF ≈ 2600 s^{-1}, is several orders of magnitude larger than that measured in organic solvents. This is however a rough estimation because first there is a strong indication that the current i_p measured at neutral pH actually corresponds to the current for the reduction of **1** coupled with a protonation step and second the catalytic waves are rather peak shaped than S-shaped as would be expected from the theory. Note however that our electrochemical measurements are consistent with the high rate of photochemical hydrogen production previously obtained with a bdt diiron derivative in a 1 : 1 DMF/water mixture.[22]

3.3. Bulk electrolysis of acid solutions of 1

To confirm the catalytic efficiency of **1**, electrolysis was carried out at −0.66 V on a mercury pool electrode in the presence

of a large excess of acetic acid ([**1**] = 8 μM, [HOAc] = 50 mM, pH 3.0). Formation of gas bubbles could be observed and evolution of H_2 was confirmed by gas chromatography. The charge accumulated over a period of one hour, after correction from the contribution of the blank solution, results in a turnover number (TON) of 52 moles of H_2 per mole of **1** (Fig. S5, ESI†). This TON value is a conservative underestimate that could be significantly increased by the utilisation of a larger separation frit and optimization of the cell surface area to volume ratio.

Since two protons are consumed for each H_2 molecule produced, measuring the increase in pH during electrolysis is an easy method to quantify the Faradaic efficiency of **1**. The rise of *ca.* 1.1 pH units observed after a 30 min electrolysis at −0.66 V of an acidified NaCl solution matches that calculated from the amount of charge consumed, establishing that **1** operates close to 100% Faradaic efficiency (Fig. S6, ESI†).

Polarogram and UV-visible spectrum recorded after electrolysis indicated no noticeable degradation of **1**. Control experiment showed a low catalytic activity when a fresh acidic electrolyte that does not contain **1** was added to a used mercury pool electrode rinsed once with water, indicating a slight adsorption of **1** during electrolysis (Fig. S5, ESI†). However no solid deposits were observed on the mercury surface, which remained shiny after extended experiments.

3.4. Mechanism of catalytic H_2 production mediated by 1

Electrochemical measurements described above parallel those carried out in organic solvents. A practical advantage of working in an aqueous medium is that not only acid concentration but also pH can be easily altered. We evaluated the pH effect on the current–potential response of **1** by varying the relative proportion of H_3PO_4, H_2PO4^- and $HPO4^{2-}$ while maintaining the total concentration of the electrolyte at 0.1 M (Fig. 5). Decreasing pH from 7.1 to 2.8 shifts positively the peak potential, consistent with an electrochemical reduction that involves protons. The slope $\partial E/\partial pH = 30$ mV ($\sim$2.3 RT/2F) suggests that the transfer of one proton is coupled to the transfer of two electrons. The peak current is not very responsive to pH over the range 7 to 6. The potential of the reduction peak shifts however positively, showing that the reduction of **1** is coupled with proton transfer even at neutral pH. The catalytic current increases by two orders of magnitude over the range $6 > pH > 3$. This clearly indicates that the rate determining step of H_2 production is a protonation step. We also note that the catalytic current tends to level off at $pH < 3$, likely because of a change in the catalytic mechanism.

From these results and on the basis of literature precedent, we tentatively propose the catalytic cycle depicted in Scheme 2. Catalysis begins with the reduction of the binuclear Fe^IFe^I compound **1**. Whether this reduction step involves two electrons as seen in organic solvents or only one electron is not established. In both situations, the electron transfer steps are coupled with a proton transfer step (oxidative addition of H^+) leading to the putative hydride intermediate $[Fe^0–Fe^{II}(H)]^-$. In organic solvents, this Fe^0Fe^{II}-hydride intermediate is hardly protonated by strong acid, which explains the poor activity of **1** for H_2 production in acetonitrile for example. In contrast, in aqueous media, the Fe^0Fe^{II}-hydride intermediate is protonated at $pH < 6$ to release H_2 regenerating **1** and closing the catalytic cycle.

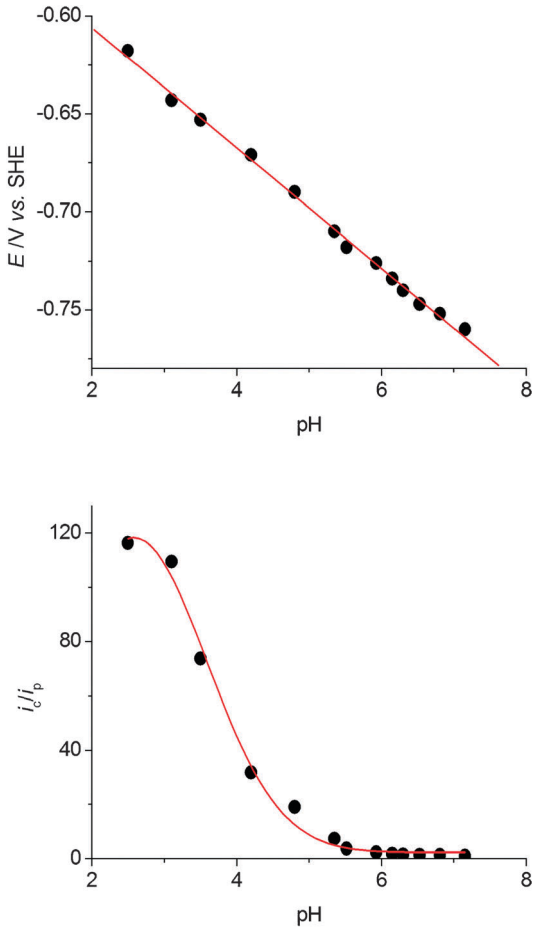

Fig. 5 Plots of the catalytic wave potential (top) and current enhancement (bottom) *versus* pH measured for 20 μM **1** in 0.1 M phosphate solution containing 10 mM SDS. pH was adjusted by varying the relative proportion of H_3PO_4, H_2PO4^- and $HPO4^{2-}$. Peak potential and current were obtained by differential pulse polarography at a scan rate of 2.5 mV s^{-1} and an amplitude of 50 mV.

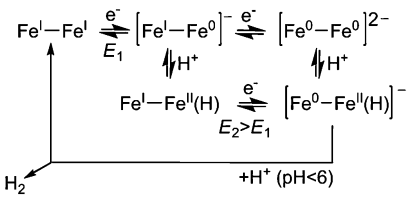

Scheme 2 Proposed mechanism for the catalysis of electrochemical H_2 production mediated by **1**.

We postulate that the last protonation step is the rate determining step in agreement with the pH dependence of the catalytic current (Fig. 4).

4. Conclusions

In summary, we showed that the hydrophobic bdt-diiron derivative **1** can be easily dispersed in an aqueous SDS solution. Reproducible current–potential responses corresponding to the reduction of freely diffusing species were obtained over a large pH range at a dropping mercury electrode. The most striking result is the high catalytic activity of **1** for H_2 production in

water regarding its poor catalytic activity for the same reaction in organic solvent. Beyond the questions raised regarding the validity and relevance of the TOF value (2600 s^{-1} at [acid] = 10 mM) obtained here by the Dubois's treatment, the high activity of the bdt-diiron catalyst is clearly demonstrated by observation of current densities exceeding 0.5 mA cm^{-2} at [**1**] = 60 μM and [acid]/[**1**] = 17. Another important result is that the bdt-diiron derivative **1** works at potentials positive to −0.7 V at pH ≈ 3, corresponding to an overpotential $|\eta| < 0.5$ V that is competitive with those recently reported for the molecular cobalt pyridine catalysts producing H_2 at neutral pH.[34,35]

Furthermore, the electrochemical method described in this paper should permit extended investigation of diiron models in water without complications brought in by the synthesis of compounds holding hydrophilic ligands.

Acknowledgements

This work was supported by Agence Nationale de la Recherche (ANR) through the program "TECH'BIOPHYP", Centre Nationale de la Recherche Scientifique (CNRS) and Université de Bretagne Occidentale.

Notes and references

1 G. W. Crabtree, M. S. Dresselhaus and M. V. Buchanan, *Phys. Today*, 2004, **57**, 39–44.
2 J. A. Turner, *Science*, 2004, **305**, 972–974.
3 N. S. Lewis and D. G. Nocera, *Proc. Natl. Acad. Sci. U. S. A.*, 2006, **103**, 15729–15735.
4 L. Hammarstrom and M. R. Wasielewski, *Energy Environ. Sci.*, 2011, **4**, 2339–2339.
5 C. Herrero, A. Quaranta, W. Leibl, A. W. Rutherford and A. Aukauloo, *Energy Environ. Sci.*, 2011, **4**, 2353–2365.
6 U. Koelle and S. Paul, *Inorg. Chem.*, 1986, **25**, 2689–2694.
7 V. Artero, M. Chavarot-Kerlidou and M. Fontecave, *Angew. Chem., Int. Ed.*, 2011, **50**, 7238–7266.
8 D. L. DuBois and R. M. Bullock, *Eur. J. Inorg. Chem.*, 2011, 1017–1027.
9 Y. Nicolet, B. J. Lemon, J. C. Fontecilla-Camps and J. W. Peters, *Trends Biochem. Sci.*, 2000, **25**, 138–143.
10 R. K. Thauer, *Eur. J. Inorg. Chem.*, 2011, 919–921.
11 J.-F. Capon, F. Gloaguen, P. Schollhammer and J. Talarmin, *Coord. Chem. Rev.*, 2005, **249**, 1664–1676.
12 F. Gloaguen and T. B. Rauchfuss, *Chem. Soc. Rev.*, 2009, **38**, 100–108.
13 C. Tard and C. J. Pickett, *Chem. Rev.*, 2009, **109**, 2245–2274.
14 M. Wang, L. Chen, X. Li and L. Sun, *Dalton Trans.*, 2011, **40**, 12793–12800.
15 G. A. N. Felton, C. A. Mebi, B. J. Petro, A. K. Vannucci, D. H. Evans, R. S. Glass and D. L. Lichtenberger, *J. Organomet. Chem.*, 2009, **694**, 2681–2699.
16 X. Liu, X. Ru, Y. Li, K. Zhang and D. Chen, *Int. J. Hydrogen Energy*, 2011, **36**, 9612–9619.
17 R. Mejia-Rodriguez, D. Chong, J. H. Reibenspies, M. P. Soriaga and M. Y. Darensbourg, *J. Am. Chem. Soc.*, 2004, **126**, 12004–12014.
18 Y. Na, M. Wang, K. Jin, R. Zhang and L. Sun, *J. Organomet. Chem.*, 2006, **691**, 5045–5051.
19 U.-P. Apfel, Y. Halpin, M. Gottschaldt, H. Görls, J. G. Vos and W. Weigand, *Eur. J. Inorg. Chem.*, 2008, 5112–5118.
20 M. L. Singleton, J. H. Reibenspies and M. Y. Darensbourg, *J. Am. Chem. Soc.*, 2010, **132**, 8870–8871.
21 M. L. Singleton, D. J. Crouthers, R. P. Duttweiler, J. H. Reibenspies and M. Y. Darensbourg, *Inorg. Chem.*, 2011, **50**, 5015–5026.
22 D. Streich, Y. Astuti, M. Orlandi, L. Schwartz, R. Lomoth, L. Hammarström and S. Ott, *Chem.–Eur. J.*, 2010, **16**, 60–63.
23 F. Wang, W.-G. Wang, X.-J. Wang, H.-Y. Wang, C.-H. Tung and L.-Z. Wu, *Angew. Chem., Int. Ed.*, 2011, **50**, 3193–3197.
24 H.-Y. Wang, W.-G. Wang, G. Si, F. Wang, C.-H. Tung and L.-Z. Wu, *Langmuir*, 2010, **26**, 9766–9771.
25 A. E. Kaifer and A. J. Bard, *J. Phys. Chem.*, 1985, **89**, 4876–4880.
26 J. S. McKennis and E. P. Kyba, *Organometallics*, 1983, **2**, 1249–1251.
27 G. A. N. Felton, A. K. Vannucci, J. Chen, L. T. Lockett, N. Okumura, B. J. Petro, U. I. Zakai, D. H. Evans, R. S. Glass and D. L. Lichtenberger, *J. Am. Chem. Soc.*, 2007, **129**, 12521–12530.
28 J.-F. Capon, F. Gloaguen, P. Schollhammer and J. Talarmin, *J. Electroanal. Chem.*, 2004, **566**, 241–247.
29 J.-F. Capon, F. Gloaguen, P. Schollhammer and J. Talarmin, *J. Electroanal. Chem.*, 2006, **595**, 47–52.
30 J. A. Cabeza, M. A. Martinez-Garcia, V. Riera, D. Ardura and S. Garcia-Granda, *Organometallics*, 1998, **17**, 1471–1477.
31 Y. Sano, A. Onoda and T. Hayashi, *Chem. Commun.*, 2011, **47**, 8229–8231.
32 J. Aušra, J. A. Wright and C. J. Pickett, *Eur. J. Inorg. Chem.*, 2011, 1033–1037.
33 M. L. Helm, M. P. Stewart, R. M. Bullock, M. R. DuBois and D. L. DuBois, *Science*, 2011, **333**, 863–866.
34 B. D. Stubbert, J. C. Peters and H. B. Gray, *J. Am. Chem. Soc.*, 2011, **133**, 18070–18073.
35 Y. Sun, J. P. Bigi, N. A. Piro, M. L. Tang, J. R. Long and C. J. Chang, *J. Am. Chem. Soc.*, 2011, **133**, 9212–9215.